



Contents lists available at ScienceDirect

Journal of King Saud University – Science

journal homepage: www.sciencedirect.com

Original article

Influence of surfactants and surfactant-coated IONs on the rate of alkaline hydrolysis of procaine in the presence of PEG

Kashif Raees, Mohd Shaban Ansari, M.Z.A. Rafiquee*

Department of Applied Chemistry, Zakir Hussain College of Engineering and Technology, Aligarh Muslim University, Aligarh 202002, UP, India

ARTICLE INFO

Article history:

Received 9 August 2019

Revised 25 September 2019

Accepted 5 November 2019

Available online 20 November 2019

Keywords:

Hydrolysis of procaine

Magnetic nanoparticles

Surfactant-coated iron oxide nanoparticles

Polymer-surfactant aggregates

ABSTRACT

The influence of surfactant coated iron oxide nanocomposites (Surf-IONs) and surfactants on the rate of alkaline hydrolysis of procaine hydrochloride (2-diethylaminoethyl-4-aminobenzoic acid) in the presence of poly(ethylene glycol) (PEG) have been investigated under the varying reaction conditions. The nanoparticles were synthesised using the co-precipitation method and were characterised using X-ray diffraction (XRD), Fourier transform infrared spectroscopy (FTIR), Vibrating sample magnetometer (VSM) and Thermogravimetric analysis (TGA). The concentration of NaOH was taken in overabundance over [procaine] for maintaining the reactions under pseudo-first-order conditions. The kinetic effect of poly(ethylene glycol); PEG of molecular weights 1500, 4000, 6000, and 8000 with the cetyltrimethylammonium bromide; CTABr and sodium dodecyl sulphate; SDS (either free or coated on iron oxide nanoparticles) were studied. A fall in the values of the rate constant on increasing the [surfactant] or [Surf-IONs] at fixed [PEG] was observed. The k_p -[PEG-surfactant] profile was treated using the pseudophase model, and pseudophase ion exchange model and the kinetic parameters were determined. The binding constant of procaine with PEG-surfactant aggregates was found to be lower than the respective micelles in the absence of PEG. The increase in the molecular weights of PEG decreased the values of binding constants and equilibrium constants.

© 2019 The Author(s). Published by Elsevier B.V. on behalf of King Saud University. This is an open access article under the CC BY-NC-ND license (<http://creativecommons.org/licenses/by-nc-nd/4.0/>).

1. Introduction

The nano-sized materials have been extensively investigated in the last two decades because they owe superior physical as well as chemical properties due to their small object effect, quantum size effect, mesoscopic effect and the surface effect, as compared to their bulk counterparts (Wei et al., 2012). The nano-materials have applications in almost every field of science and technology like everyday materials and processes, biomedical applications, electronic and IT applications, and environmental remediation (Matsui, 2005; Nikitin et al., 2017; Prasad et al., 2018). Among all the nanoparticles or nanocomposites, the iron oxide nanoparticles (IONs) has drawn the attention because it is almost inexpensive, biocompatible, inert, having high magnetism, recoverable or

separable using simple magnets and are reusable or recyclable (Alishiri et al., 2013; Godoi et al., 2014). IONs have applications in magnetic fluids, magnetic seals, chemical catalysis and data storage (Azharuddin et al., 2008; Frey et al., 2009; Mamani et al., 2014). The IONs are also used in clinical diagnosis and therapy (like MRI and MFH), targeted drug delivery, magnetic bioseparation and biological labels (Cole et al., 2011; Yue-jian et al., 2010). The other advantages with IONs are that its size, shape, and morphology can be controlled as per the requirement of the application during the synthesis process (Shen et al., 2014).

The IONs are sometimes coated with materials like polymers, surfactants, organics (like oleic acid) and inorganics (like silica) to improve its properties like lowering the self-aggregation ability, and increasing the stability (Illés et al., 2015; Mahdavi et al., 2013; Maleki et al., 2019; Santra et al., 2001). The IONs usually coated with polymers and more often with natural polymers like Polyethylene glycol (PEG), Chitosan, Polyacrylic acid (PAA) and starch to lower the toxicity and also to reduce the self-aggregation (Mukhopadhyay et al., 2012; Pham et al., 2016; Sanchez et al., 2018). The complex behaviour of polymer-surfactant interactions has the property to alter the viscosity, wettability, detergency and foaming behaviour of a solution (Mace et al., 2012; Schramm et al., 2003). The polymer-surfactant aggregates have a smaller size

* Corresponding author.

E-mail address: drrafiquee@yahoo.com (M.Z.A. Rafiquee).
Peer review under responsibility of King Saud University.

Production and hosting by Elsevier

and a higher degree of ionisation (Rehman et al., 2013). The aggregation of polymer and surfactant is very similar to the micellization, but it takes place at a concentration higher than the critical aggregation concentration (CAC) of the surfactant which is relatively lesser than the critical micelle concentration (CMC) of the corresponding surfactant (Raees et al., 2018). Interaction between polymer and surfactant depends upon the type of surfactants; generally non-ionic polymer interacts dynamically with anionic surfactant and comparatively weaker with cationic and non-ionic surfactant, nature of interactions involved between the polymer and surfactant molecules (van Der Waals forces, hydrogen bonding, and electrostatic bond), as well as on the charge density of the polymer chain (Miyake, 2017). Physical properties like surface tension and conductivity measurements of polymer-surfactant mixtures indicate the formation of polymer-surfactant aggregate due to the cooperative binding of polymer and surfactant molecules. This binding increases with the increase in hydrophobicity of these molecules. The binding also increases by increasing surfactant concentration until all the polymer molecules get fully saturated (Manna and Panda, 2011; Tromsdorf et al., 2009). The polymer-surfactant complexes may exist in either of three different phases or stages according to their electric equivalent ratio (the number of ionised groups of surfactant divided by the number of ionised groups of polymer) present in the mixture solution. The first stage exists when the surfactant's concentration is under CMC; the surfactant ions bind cooperatively to the polymer strands. In the next stage, on increasing the surfactant concentration so that the equivalent ratio becomes equal to 1, the complex becomes insoluble and gets precipitated. On further increasing the surfactant concentration in the 3rd stage, the complex gets resubtilized and co-exist with free micelles (Pojják et al., 2011).

Procaine hydrochloride, commercially known as novocaine or 'Novocain', is an ester-based local anaesthetic drug and used commonly by dentists during dental procedures like cavity filling. It is also used in severe pain conditions like arthritis for regional anaesthesia (Reuss-Lamky, 2007). Its stability has always been an issue because of its lower shelf life. Natural polymers like PEG and surfactants found effective in lowering its rate of degradation, hence, increasing stability (Reichert and Butterworth, 2004). PEG is a natural polymer that is approved by the FDA as food and drug additives. The rate of alkaline hydrolysis of procaine in the copresence of surfactant-PEG and surfactant-IONs-PEG give an insight into the stability and binding ability of procaine with PEG under these systems. Therefore, the present studies have been undertaken to elucidate the synergistic effect of surfactant-PEG and surfactant-IONs-PEG on the stability of procaine in the presence of PEG. PEGs with molecular weight 1500, 4000, 6000 and 8000 were used to explore the role of molecular weight of PEG during the formation of surfactant-PEG complex.

2. Experimental section

2.1. Reagents

Procaine HCl (98%), obtained from TCI, Tokyo, Japan. Polyethylene glycol with molecular weight 1500, 4000, 6000, and 8000, Ferrous chloride dihydrate (99%), CTABr (99%), SDS (99%) and Ferric chloride (97%) were acquired from CDH, New Delhi, India. 25% Ammonium hydroxide solution with 99% purity was obtained from Thermo Fisher Scientific, Mumbai, India and sodium hydroxide (97%) was procured from Merck, Mumbai, India to carry out the studies.

These reagents were of analytical grade and used without further purification. The stock solution of procaine hydrochloride

was prepared in 99.9% ethanol, while all other solutions were prepared in double distilled water.

2.2. Synthesis of Surfactant-Coated iron oxide nanocomposites (Surf-IONs)

Surfactant coated magnetite nanocomposites were synthesised by mixing the surfactants (CTABr and SDS) in an appropriate amount during the co-precipitation of Fe^{3+} and Fe^{2+} salts. The ferric and ferrous salts were taken in 2:1 M ratio (Fe^{3+} ; 4.0×10^{-1} mol dm^{-3} and Fe^{2+} ; 2.0×10^{-1} mol dm^{-3}) and dissolved in 300 mL of 2.0×10^{-1} mol dm^{-3} surfactant solution taken into a 1000 mL capacity conical flask. The mixture containing FeCl_3 , $\text{FeCl}_2 \cdot 2\text{H}_2\text{O}$ and the surfactant (SDS or CTABr) was then purged with N_2 gas to remove any oxygen and stirred strenuously for an hour to ensure absolute mixing. Co-precipitation was achieved by adding 200 mL of 25% ammonium hydroxide solution (liquor ammonia) and a few mL of 2.0 mol dm^{-3} NaOH dropwise in the reaction mixture. Then the temperature of the mixture was elevated to 60 °C while continuously shaking and purging Nitrogen gas for 4 h. The precipitated magnetite nanoparticles were separated using a magnet and washed with ethanol and de-ionised water until the pH comes to neutral. The freshly prepared nanoparticles were then dispersed in the surfactant solution (CTABr or SDS), and the solution was sonicated at room temperature in an ultrasonic bath (LABMAN scientific instruments) for 30 min to ensure the maximum yield of surface-modified nanoparticles. The surfactant-coated nanocomposites were separated using a magnet and washed with acetone and de-ionised water to remove any unbound surfactant molecules and then dried for 3–4 h under vacuum and used for kinetic studies and characterisations.

The synthesised surf-IONs were characterised for FT-IR spectra using Nicolet iS50 FT-IR Spectrometer (Thermo Fisher Scientific, Madison, USA). The XRD patterns of the nanocomposites were recorded by MiniFlex II, X-ray diffractometer (Rigaku, Japan) provided with a Cu $K\alpha$ radiation source ($\lambda = 1.5406$ nm). The Thermogravimetric analyses (TGA) of the nanocomposites were done by using Pyris 1 Thermogravimetric analyser (Perkin Elmer). Vibrating sample magnetometer (VSM), MicroMag-3900 (Princeton, USA) was used to determine the magnetic character of the nanocomposites.

2.3. Kinetic measurements

The kinetic measurements were performed under the pseudo-first-order reaction conditions (i.e. $[\text{NaOH}] \gg [\text{Procaine}]$), using GENESYS 10S UV/VIS spectrophotometer (Thermo Fisher Scientific, Madison, USA). A fall in the absorbance for the hydrolysis of procaine was measured at a wavelength of 291 nm with respect to time. The absorbance of the samples was measured in a 3.0 mL quartz cuvette having a path length of 1 cm. A calculated amount of reactants, surfactants and/or surf-IONs were mixed in a 100 mL three-necked round bottom flask and held in a water bath (Ferrotek Equipments, Ghaziabad, India) to keep the temperature constant at 37.0 ± 0.2 °C for 1 h to equilibrate the mixture. The reaction initiated immediately after the introduction of NaOH into the reaction vessel. The kinetic measurements were set in the spectrophotometer at a time gap of 300 s, and the reaction was tracked until the completion of 3 half-life periods. The rate constants were determined by the slope of the plot of \ln (absorbance) versus time. Multiple kinetic runs were repeated for every set of reaction to minimize random errors, and the values of rate constants were observed to be consistent under the error limit of $\pm 5\%$.

3. Results and discussion

3.1. Characterization of Surfactant-coated iron oxide nanocomposites

3.1.1. X-ray diffraction (XRD)

Fig. 1 represents the XRD patterns of the synthesised surf-IONs, which confirm the crystalline nature of the nanocomposites. The diffraction peaks are visible at $2\theta = 30.26^\circ$ (2 2 0), 35.5° (3 1 1), 43.12° (4 0 0), 53.74° (4 2 2), 57.10° (5 1 1) and 62.92° (4 4 0). The sharp peaks signify the ultrafine nature and high crystallinity of the prepared surf-IONs having the cubic structure (Mahadevan et al., 2007).

3.1.2. Fourier transform infrared spectroscopy (FTIR)

Fig. 2 (a) and (b) show the FTIR spectra of SDS-IONs and CTABr-IONs, respectively. The peaks arising at 3431 cm^{-1} in (a) and 3430 cm^{-1} in (b) are due to O–H stretching vibration arising by the presence of moistures on the surfaces of Surf-IONs. The peaks at 2922 cm^{-1} and 2854 cm^{-1} in (a) and at 2920 cm^{-1} and 2850 cm^{-1} in (b) are assigned to CH band vibrations of the $-\text{CH}_2$ group of SDS and CTABr. The H–O–H bending of H_2O appears at 1635 cm^{-1} and 1631 cm^{-1} in (a) and (b) respectively (Saranya et al., 2015). The peaks at 1460 cm^{-1} in (a) and 1465 cm^{-1} in (b) represents the $-\text{CH}_2$ group bending vibration in SDS and CTABr. The S = O stretching vibrations peak for SDS-IONs can be seen at 1220 cm^{-1} . The peak at 964 cm^{-1} in (a), corresponds to the out-of-plane bending vibration of C–H bond. The peaks at 547 cm^{-1} and 474 cm^{-1} in (a) and 566 cm^{-1} and 475 cm^{-1} in (b) are attributed to the Fe–O bond of Fe_3O_4 and the 2 peaks confirms the spinal structure of Fe_3O_4 (Aliramaji et al., 2015). The differentiation in the Fe–O bond length in magnetite molecule is the reason for 2 peaks for Fe–O bonds.

3.1.3. Vibrating sample magnetometer (VSM)

The magnetic character of the Surf-IONs was studied using VSM and the hysteresis curve of SDS-IONs and CTABr-IONs are shown in Fig. 3. The saturation magnetisation for SDS-IONs was observed

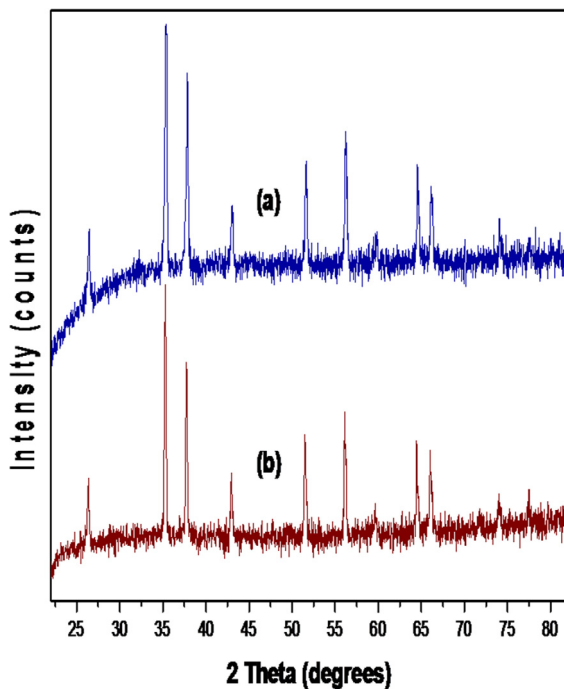


Fig. 1. XRD patterns of the synthesised SDS-IONs (a), and CTABr-IONs (b).

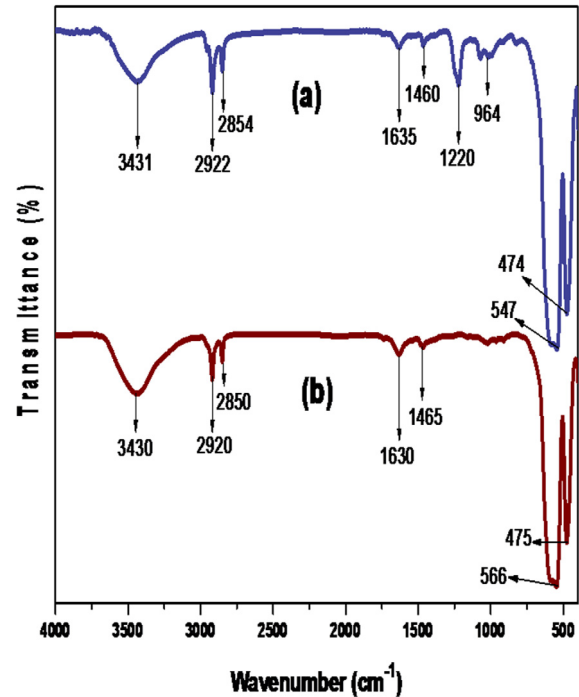


Fig. 2. FTIR spectra of the synthesised SDS-IONs (a), and CTABr-IONs (b).

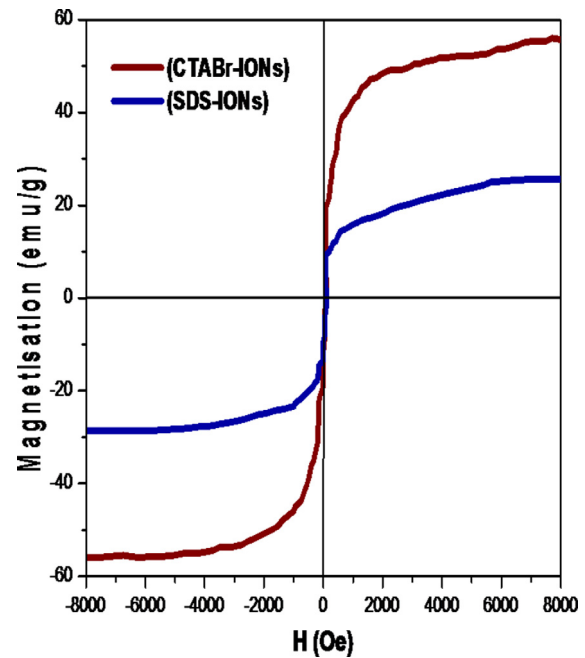


Fig. 3. Hysteresis curves at room temperature.

at 25.28 emu/g and for CTABr-IONs at 55.94 emu/g (Lu et al., 2002).

3.1.4. Thermogravimetric analysis (TGA)

The TGA curves (Fig. 4) provide the quantitative proofs for the successful coating of surfactants on the magnetite nanoparticles. The Surf-IONs were heated to 800°C and a significant weight loss occurred on increasing the temperature upto 800°C . The weight loss is attributed to the loss of organic material (surfactants) coated on the nanoparticles (El-kharrag et al., 2011; Kavas et al., 2013).

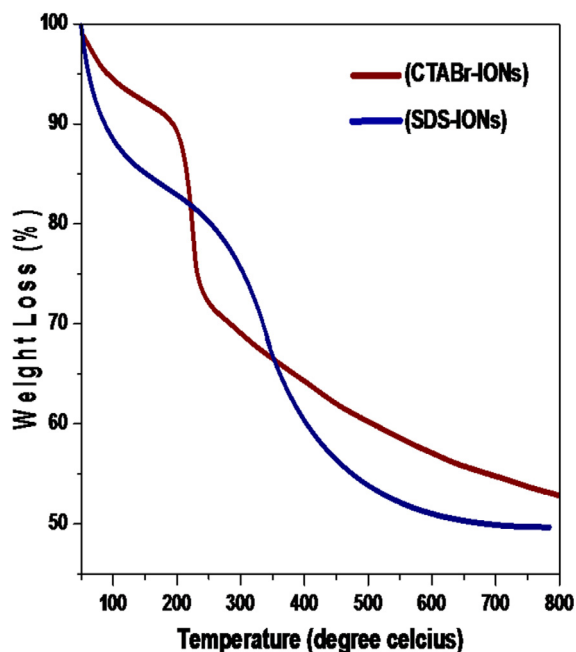


Fig. 4. TGA curves of synthesised Surf-IONs.

3.2. Influence of PEG-Surfactant aggregates on the rate of “hydrolysis of procaine”

The kinetics of the hydrolysis of procaine was performed in the copresence of 0.5% (w/v) PEG and at different concentrations of CTABr and SDS, ranging between $1.0 \times 10^{-2} \text{ mol dm}^{-3}$ to $5.0 \times 10^{-2} \text{ mol dm}^{-3}$. The rate of hydrolysis decreased in the presence of PEG on increasing the concentrations of surfactants. The rate constant values for the hydrolysis of procaine in the absence and presence of PEGs at different [surfactants] are compared in Tables 1 and 2. The rate of hydrolysis is found to be higher when the PEG is present the at respective surfactant concentration (Figs. 5 and 6). The enhancement in the rate of hydrolysis is due to the exclusion of procaine from the PEG-surfactant phase to the aqueous phase. The micellar aggregates formed by surfactant-polymer interaction is much smaller in size than the respective surfactant micelles (Shaban Ansari et al., 2018). The Necklace model suggests that the spherical structure of surfactant-polymer aggregates is compact, and polymer strands are bound with surfactant molecules (Nikas and Blankschtein, 1994). The surfactant-polymer aggregates provide a less binding opportunity for the substrate. The increase in [surfactant] in the presence of PEG excludes more and more substrates from the micellar aggregates to the aqueous phase. The increase in the chain size of PEG makes the PEG-surfactant structure more compact and results in a decrease

in the binding ability of surfactants with procaine (Mészáros et al., 2005). It is evident from the data presented in Tables 3 and 4. As the PEG and surfactant are being present in the solution, the reaction media can be divided into three distinct but homogeneous microscopic phases, namely; PEG-surfactant, micellar and aqueous pseudophases. The hydrolysis is assumed to occur in all these pseudophases. The mechanism of hydrolysis of procaine is presented in Scheme 1.

In this Scheme 1, k_p is the first-order rate constant for the hydrolysis of procaine when the PEG-surfactant aggregate is being present, $[S_p]$ is the amount of procaine attached with PEG-surfactant aggregate, OH_p^- is the amount of OH^- in the PEG-surfactant pseudophase. Similarly, the notations with subscripts ‘w’ represent the aqueous pseudophase and ‘m’ represent the micellar pseudophases. The corresponding rate equation for Scheme 1 can be represented by Eq. (1):

$$\text{Rate} = k_w[S_w] + k_p[S_p] + k_m[S_m] \quad (1)$$

The micelles and PEG-surfactant aggregates are dynamic. They are continually aggregating and disintegrating to give PEG-surfactant aggregates in equilibrium with the surfactant monomers. The surfactant molecules in the presence of polymers remain aggregated together through the cooperative binding between them through the hydrophobic interactions. It is evident from the neutron scattering studies that the surfactant molecules are located at the surface at the surface of polymer aggregates (Claesson et al., 2000; Mészáros et al., 2003). These surfactant molecules are associated with the polymers as monomers rather than in the form of micelles. Based on above theories, it is presumed that approximately the whole quantity of surfactants exists in the complexed state with PEG and an almost negligible amount of free micelles exist in the presence of PEG (Ghosh and Pandey, 1999; Rahman and Rafique, 2019). This observation is supported by the results obtained at different concentrations of PEG (from 0.5% to 2.5% (w/v)), in which the values of rate constant was almost in the similar range (Table 5). Thus, the Eq. (1) takes the form of Eq. (2):

$$\text{Rate} = k_w[S_w] + k_p[S_p] \quad (2)$$

In the presence of PEG and surfactants, equilibrium exists between the procaine molecules associated with PEG-surfactant (S_p) and free procaine molecules distributed in the aqueous phase (S_w). This equilibrium distribution can be represented by Eq. (3) as follows:



Here, $[PD_n]$ is the micellized surfactant with PEG.

K_p is the equilibrium constant and given by Eq. (4).

$$K_p = \frac{[S_p]}{[PD_n][S_w]} \quad (4)$$

Table 1

Values of rate constants in the presence of CTABr and CTABr-PEG.

[CTABr] (10^2 mol dm^{-3})	$(10^4 k_p \text{ (s}^{-1}\text{)})$				
	CTABr ^a	CTABr and PEG1500 ^b	CTABr and PEG4000 ^b	CTABr and PEG6000 ^b	CTABr and PEG8000 ^b
1.0	3.08	3.11	3.15	3.22	3.29
2.0	2.17	2.42	2.49	2.69	2.78
3.0	1.89	2.11	2.18	2.44	2.57
4.0	1.43	1.62	1.74	1.98	2.13
5.0	1.07	1.19	1.41	1.78	1.91

Reaction conditions: [Procaine] = $5.0 \times 10^{-5} \text{ mol dm}^{-3}$, [NaOH] = $5.0 \times 10^{-2} \text{ mol dm}^{-3}$, PEG = 0.5% (w/v) and Temperature = 37 °C.

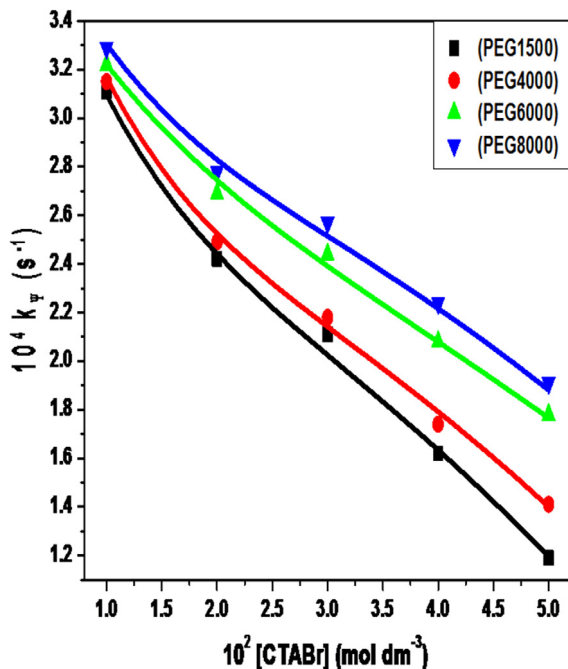
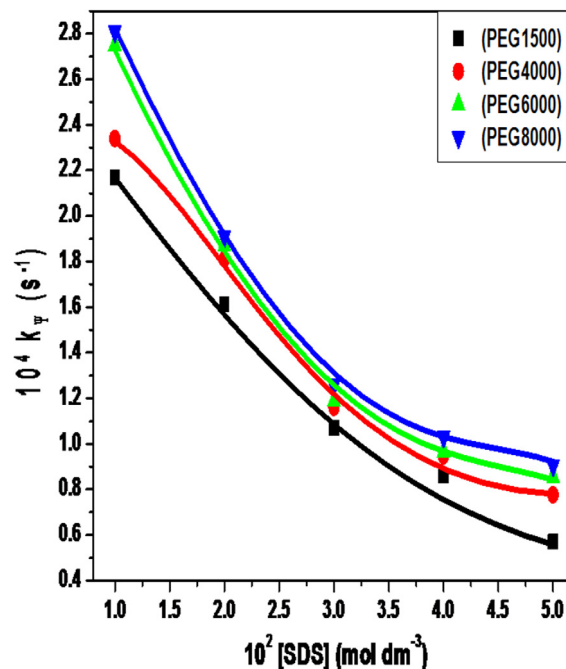
^a Reference No. 36.

^b Present Work.

Table 2

Values of rate constants in presence of SDS and SDS-PEG.

[SDS] (10^2 mol dm^{-3})	$(10^4 k_{\psi} \text{ (s}^{-1}\text{)})$				
	SDS ^a	SDS and PEG1500 ^b	SDS and PEG4000 ^b	SDS and PEG6000 ^b	SDS and PEG8000 ^b
1.0	0.91	2.17	2.34	2.75	2.81
2.0	0.65	1.61	1.81	1.87	1.91
3.0	0.53	1.07	1.16	1.19	1.26
4.0	0.44	0.86	0.95	0.97	1.03
5.0	0.27	0.57	0.78	0.86	0.91

Reaction conditions: [Procaine] = $5.0 \times 10^{-5} \text{ mol dm}^{-3}$, [NaOH] = $5.0 \times 10^{-2} \text{ mol dm}^{-3}$, PEG = 0.5% (w/v) and Temperature = 37 °C.^a Reference No. 36^b Present Work**Fig. 5.** Plots of k_{ψ} versus [CTABr] in the presence of PEGs. Reaction conditions: [Procaine] = $5.0 \times 10^{-5} \text{ mol dm}^{-3}$, [NaOH] = $5.0 \times 10^{-2} \text{ mol dm}^{-3}$, [PEG] = 0.5% w/v and Temperature = 37 °C.**Fig. 6.** Plots of k_{ψ} versus [SDS] in the presence of PEGs. Reaction conditions: [Procaine] = $5.0 \times 10^{-5} \text{ mol dm}^{-3}$, [NaOH] = $5.0 \times 10^{-2} \text{ mol dm}^{-3}$, [PEG] = 0.5% w/v and Temperature = 37 °C.

The rate of reaction in terms of total procaine [S_T] ($=[S_w] + [S_p]$) is given by Eq. (5).

$$\text{Rate} = \frac{K_w + K_p K_p [PD_n]}{1 + K_p [PD_n]} [S_T] = k_{\psi} [S_T] \quad (5)$$

Or,

$$k_{\psi} = \frac{K_w + k_p K_p [PD_n]}{1 + K_p [PD_n]} \quad (6)$$

For PEG-CTABr aggregates

$$K_{Br}^{OH} = \frac{[OH_p^-][Br_w^-]}{[OH_w^-][Br_p^-]} \quad (7)$$

The rate Eq. (7) in terms of K_p , k_w and k_p can be written as (Eq. (8)):

$$k_{\psi} = \frac{k_2 [OH_T^-] + (k_p K_p - k_2) m_{OH} [PD_n]}{1 + K_p [PD_n]} \quad (8)$$

The values of k_p and K_p were determined by the iterations method as described in the literatures (Menger and Portnoy, 1967; Raees et al., 2019; Rodenas and Vera, 1985) and the obtained values are given in Table 1.

Table 3Values of K_p and k'_p obtained from the plots of $\frac{1}{k_w - k_{\psi}}$ versus $\frac{1}{[PD_n]}$ for 0.5% (w/v) polyethylene glycol of different molecular weights in the presence of SDS.

Molecular weight of PEG	K_p	$10^4 k'_p \text{ (s}^{-1}\text{)}$
1500	1050	1.10
4000	887	1.27
6000	620	1.42
8000	432	1.40

Reaction conditions: [Procaine] = $5.0 \times 10^{-5} \text{ mol dm}^{-3}$, [NaOH] = $5.0 \times 10^{-2} \text{ mol dm}^{-3}$ and Temperature = 37 °C.

Eq. (9) relates the rate of hydrolysis of procaine occurring in the copresence of PEG-SDS system:

$$\frac{1}{k'_w - k_{\psi}} = \frac{1}{k'_w - k'_p} + \frac{1}{(k'_w - k'_p) K_p [PD_n]} \quad (9)$$

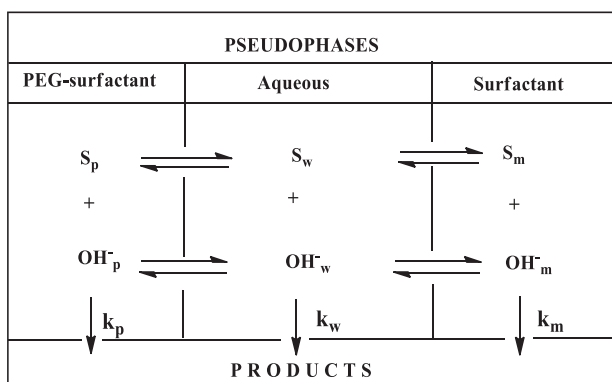
In Eq. (9), k'_w and k'_p are the first order rate constant for the hydrolysis of procaine in the aqueous and PEG-SDS pseudophases, respectively. $[PD_n]$ denotes the equilibrium concentration of PEG-surfactants complex. The values of k'_p and K_p were acquired by the plot of $\frac{1}{k'_w - k_{\psi}}$ versus $\frac{1}{[PD_n]}$, and presented in Table 2.

Table 4

Fitting values of K_p and k_p obtained from the plots of k_p versus $[PD_n]$ for CTABr in the presence of 0.5% (w/v) polyethylene glycol of different molecular weights. Kinetic parameters used for calculations, $K_{Br}^{OH} = 14$, $\beta = 0.8$, and $k_2 = 8.76 \times 10^{-3} \text{ mol}^{-1} \text{ dm}^3 \text{ s}^{-1}$.

Molecular weight of PEG	K_p	$10^4 k_p (\text{mol}^{-1} \text{ dm}^3 \text{ s}^{-1})$	cmc $10^4 (\text{mol dm}^{-3})$
1500	1680	8.72	9.0
4000	1600	9.01	9.2
6000	1000	10.60	9.3
8000	850	10.80	9.4

Reaction conditions: $[\text{Procaine}] = 5.0 \times 10^{-5} \text{ mol dm}^{-3}$, $[\text{NaOH}] = 5.0 \times 10^{-2} \text{ mol dm}^{-3}$ and Temperature = 37 °C.

**Scheme 1.**

3.3. Influence of surfactant-coated iron oxide nanocomposites (Surf-IONs) on the “hydrolysis of procaine” in the copresence of PEGs

The introduction of Surf-IONs during the reaction of procaine with NaOH lowered the rate of hydrolysis of procaine. A fall in the rate of hydrolysis was observed more pronounced in the presence of Surf-IONs than bare Fe_3O_4 . The alkaline hydrolysis of procaine in the copresence of PEGs of molecular weight 1500, 4000, 6000 and 8000 was performed at varying amount of Surf-IONs (from 0.02% to 0.40% w/v), at fixed $[\text{NaOH}]$ ($5.0 \times 10^{-2} \text{ mol dm}^{-3}$) and fixed $[\text{PEGs}]$ (0.5% w/v). Figs. 7 and 8 show that the values of rate constant decreased on increasing the $[\text{Surf-IONs}]$. It was observed that the rate constants were comparatively higher in the presence of PEG than in the absence of PEG at fixed $[\text{Surf-IONs}]$, which might be due to the hydrophobic interaction between the PEG and coated surfactant molecules. It makes it difficult for procaine molecules to cross the bulky PEG molecules, and therefore, procaine largely remains in the aqueous phase. The binding and adsorption of procaine with Surf-IONs become difficult, and so the higher rate of reaction is observed when the PEG is present. Following is the mechanism (Scheme 2) that describes the reaction in the copresence of Surf-IONs and PEG:

Table 5

Values of rate constants obtained at varying concentration of PEGs at fixed surfactants concentration.

[PEG] %(w/v)	$(10^4 k_p (\text{s}^{-1}))$							
	CTABr and PEG1500	SDS and PEG1500	CTABr and PEG4000	SDS and PEG4000	CTABr and PEG6000	SDS and PEG6000	CTABr and PEG8000	SDS and PEG8000
0.5	1.2	0.57	1.21	0.78	1.88	0.86	1.91	0.91
1.0	1.5	0.63	1.43	0.83	1.61	0.61	1.56	1.01
1.5	1.43	0.50	1.53	0.61	1.57	0.73	1.44	1.06
2.0	1.45	0.71	1.51	0.82	1.57	0.62	1.44	0.98
2.5	1.36	0.77	1.47	0.75	1.72	0.64	1.52	0.86

Reaction conditions: $[\text{Procaine}] = 5.0 \times 10^{-5} \text{ mol dm}^{-3}$, $[\text{NaOH}] = 5.0 \times 10^{-2} \text{ mol dm}^{-3}$, $[\text{surfactants}] = 5.0 \times 10^{-2} \text{ mol dm}^{-3}$ and Temperature = 37 °C.

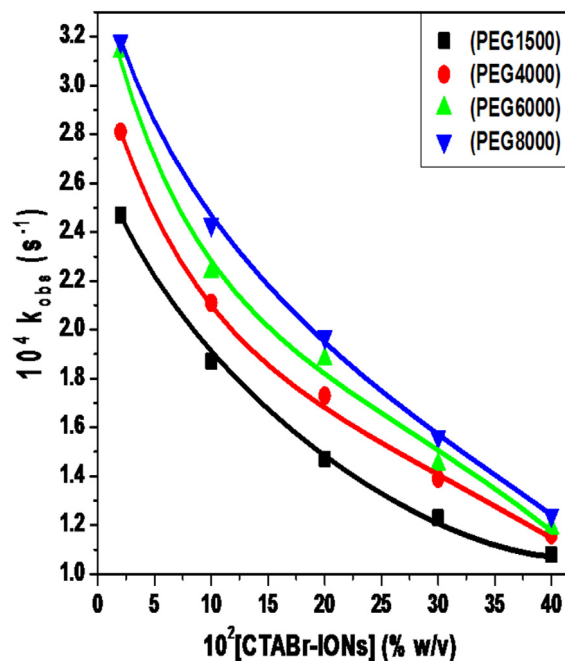


Fig. 7. Plots of k_{obs} versus $[\text{CTABr-IONs}]$ in the presence of PEGs. Reaction conditions: $[\text{Procaine}] = 5.0 \times 10^{-5} \text{ mol dm}^{-3}$, $[\text{NaOH}] = 5.0 \times 10^{-2} \text{ mol dm}^{-3}$, $[\text{PEG}] = 0.5\% \text{ w/v}$ and Temperature = 37 °C.

The increase in $[\text{Surf-IONs}]$ to the solutions containing procaine and hydroxide ions decreased the rate of reaction progressively. This observation supports the compartmentalization of reactants into two different pseudophases i.e. procaine is associated with Surf-IONs while hydrophilic OH^- ions remains in aqueous phase. Therefore, the Eq. (9) based on the pseudophase model has been used in the form of Eq. (10) to determine the equilibrium constant (K_e) for the binding between procaine and Surf-IONs.

$$\frac{1}{k'_w - k'_{\text{Surf-IONs}}} = \frac{1}{k'_w - k'_{\text{Surf-IONs}}} + \frac{1}{(k'_w - k'_m)K_e[\text{Surf-IONs}]} \quad (10)$$

The values of the rate constant ($k'_{\text{Surf-IONs}}$) for the hydrolysis of procaine in the copresence of Surf-IONs and PEG were calculated from the plot of $\frac{1}{k'_w - k'_{\text{Surf-IONs}}}$ versus $\frac{1}{[\text{Surf-IONs}]}$. The values of equilibrium constant (K_e) were obtained from the slopes of the above plots. These values are given in Tables 6 and 7.

A close observation from the Figs. 7 and 8 displays that the increase in the molecular weight of the polyethylene glycol increases the rate of reactions for both the nanoparticles (CTABr-IONs and SDS-IONs). The values of K_e , (given in Tables 6 and 7) decreases on increasing the molecular weights of the PEG in the copresence of CTABr-IONs and SDS-IONs. The higher molecular weights PEG wraps the CTABr-IONs and SDS-IONs more

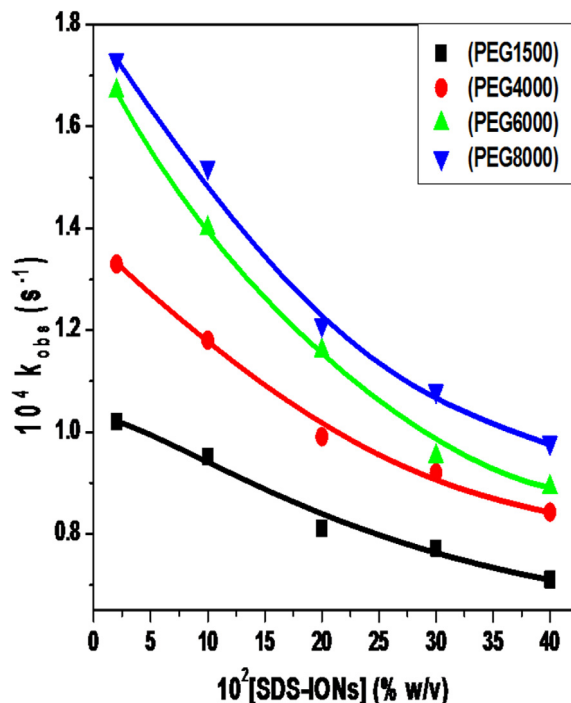


Fig. 8. Plots of k_{obs} versus [SDS-IONS] in the presence of PEGs. Reaction conditions: [Procaine] = 5.0×10^{-5} mol dm^{-3} , [NaOH] = 5.0×10^{-2} mol dm^{-3} , [PEG] = 0.5% w/v and Temperature = 37 °C.

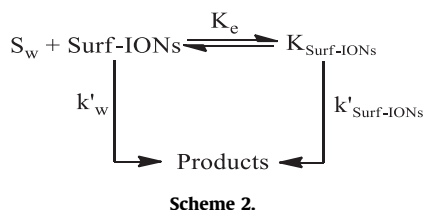


Table 6

Values of K_e obtained from the plots of $\frac{1}{k_w - k_{\text{CTABr-IONS}}}$ versus $\frac{1}{[\text{CTABr-IONS}]}$ in the presence of PEGs of different molecular weight.

CTABr-IONS with PEG	K_e	$10^5 k_{\text{CTABr-IONS}}$
PEG1500	22.1	7.53
PEG4000	16.7	7.94
PEG6000	14.1	7.82
PEG8000	10.9	6.82

Reaction conditions: [Procaine] = 5.0×10^{-5} mol dm^{-3} , [NaOH] = 5.0×10^{-2} mol dm^{-3} , [PEG] = 0.5% w/v and Temperature = 37 °C.

Table 7

Values of K_e obtained from the plots of $\frac{1}{k_w - k_{\text{SDS-IONS}}}$ versus $\frac{1}{[\text{SDS-IONS}]}$ in the presence of PEGs of different molecular weight.

SDS-IONS with PEG	K_e	$10^5 k_{\text{SDS-IONS}}$
PEG1500	112.0	6.85
PEG4000	72.6	7.44
PEG6000	42.0	7.08
PEG8000	38.4	7.80

Reaction conditions: [Procaine] = 5.0×10^{-5} mol dm^{-3} , [NaOH] = 5.0×10^{-2} mol dm^{-3} , [PEG] = 0.5% w/v and Temperature = 37 °C.

compactly and favours the equilibrium concentration of procaine molecules more into the aqueous phase and therefore, the higher rate constant values are observed.

4. Conclusion

The introduction of polyethylene glycols with molecular weight 1500, 4000, 6000 and 8000 to the reaction mixture having surfactants/surfactant coated iron oxide nanocomposites suppressed the rate of hydrolysis of procaine. The pseudophase ion-exchange model is validated to determine the kinetic parameters in the copresence of PEG-CTABr aggregates. The hydrolysis in the copresence of PEG-SDS aggregates followed the pseudophase model. The values of binding constant decreased on increasing the molecular weight of PEGs. Surf-IONS in the presence of PEG displayed higher values of the rate of hydrolysis than the rates of reactions obtained in the absence of PEG. The rate of reaction increased with the increase in the molecular weight of PEG.

Declaration of Competing Interest

The authors declare that they have no known competing financial interests or personal relationships that could have appeared to influence the work reported in this paper.

References

- Aliramaji, S., Zamanian, A., Sohrabijam, Z., 2015. Characterization and synthesis of magnetite nanoparticles by innovative sonochemical method. *Procedia Mater. Sci.* 11, 265–269. <https://doi.org/10.1016/j.mspro.2015.11.022>.
- Alishiri, T., Oskooei, H.A., Heravi, M.M., 2013. Fe₃O₄ nanoparticles as an efficient and magnetically recoverable catalyst for the synthesis of α , β -unsaturated heterocyclic and cyclic ketones under solvent-free conditions. *Synth. Commun.* 43, 3357–3362. <https://doi.org/10.1080/00397911.2013.786089>.
- Azharuddin, M., Tsuda, H., Wu, S., Sasaoka, E., 2008. Catalytic decomposition of biomass tars with iron oxide catalysts. *Fuel* 87, 451–459. <https://doi.org/10.1016/j.fuel.2007.06.021>.
- Claesson, P.M., Bergström, M., Dedinaite, A., Kjellin, M., Legrand, J.F., Grillo, I., 2000. Mixtures of cationic polyelectrolyte and anionic surfactant studied with small-angle neutron scattering. *J. Phys. Chem. B* 104, 11689–11694. <https://doi.org/10.1021/jp0022961>.
- Cole, A.J., David, A.E., Wang, J., Galbán, C.J., Hill, H.L., Yang, V.C., 2011. Polyethylene glycol modified, cross-linked starch-coated iron oxide nanoparticles for enhanced magnetic tumor targeting. *Biomaterials* 32, 2183–2193. <https://doi.org/10.1016/j.biomaterials.2010.11.040>.
- El-kharrag, R., Amin, A., Greish, Y.E., 2011. Synthesis and characterization of mesoporous sodium dodecyl sulfate-coated magnetite nanoparticles. *J. Ceram. Sci. Technol.* 2, 203–210. <https://doi.org/10.4416/JCST2011-00021>.
- Frey, N.A., Peng, S., Cheng, K., Sun, S., 2009. Magnetic nanoparticles: synthesis, functionalization, and applications in bioimaging and magnetic energy storage. *Chem. Soc. Rev.* 38, 2532–2542. <https://doi.org/10.1039/b815548h>.
- Ghosh, K.K., Pandey, A., 1999. Kinetic effects of surfactant/polymer mixtures upon acidic hydrolysis of hydroxamic acids. *J. Dispers. Sci. Technol.* 20, 1635–1646. <https://doi.org/10.1080/01932699908943878>.
- Godoi, M., Liz, D.G., Ricardo, E.W., Rocha, M.S.T., Azeredo, J.B., Braga, A.L., 2014. Magnetite (Fe₃O₄) nanoparticles: An efficient and recoverable catalyst for the synthesis of alkynyl chalcogenides (selenides and tellurides) from terminal acetylenes and diorganyl dichalcogenides. *Tetrahedron* 70, 3349–3354. <https://doi.org/10.1016/j.tet.2013.09.095>.
- Illés, E., Tombácz, E., Szekeres, M., Tóth, I.Y., Szabó, Á., Iván, B., 2015. Novel carboxylated PEG-coating on magnetite nanoparticles designed for biomedical applications. *J. Magn. Magn. Mater.* 380, 132–139. <https://doi.org/10.1016/j.jmmm.2014.10.146>.
- Kavas, H., Günay, M., Baykal, A., Toprak, M.S., Sozeri, H., Aktaş, B., 2013. Negative permittivity of polyaniline-Fe₃O₄ nanocomposite. *J. Inorg. Organomet. Polym. Mater.* 23, 306–314. <https://doi.org/10.1007/s10904-012-9776-7>.
- Lu, Y., Yin, Y., Mayers, B.T., Xia, Y., 2002. Modifying the surface properties of superparamagnetic iron oxide nanoparticles through A Sol–Gel approach. *Nano Lett.* 2, 183–186. <https://doi.org/10.1021/nl015681q>.
- Mace, C.R., Akbulut, O., Kumar, A.A., Shapiro, N.D., Derda, R., Patton, M.R., Whitesides, G.M., 2012. Aqueous multiphase systems of polymers and surfactants provide self-assembling step-gradients in density. *J. Am. Chem. Soc.* 134, 9094–9097. <https://doi.org/10.1021/ja303183z>.
- Mahadevan, S., Gnanaprakash, G., Philip, J., Rao, B.P.C., Jayakumar, T., 2007. X-ray diffraction-based characterization of magnetite nanoparticles in presence of goethite and correlation with magnetic properties. *Phys. E Low-dimensional Syst. Nanostructures* 39, 20–25. <https://doi.org/10.1016/j.physe.2006.12.041>.
- Mahdavi, M., Ahmad, M. Bin, Haron, J., Namvar, F., Nadi, B., Zaki, M., Rahman, A., Amin, J., 2013. Synthesis, surface modification and characterisation of biocompatible magnetic iron oxide nanoparticles for biomedical applications. *Mol.* 2013 (18), 7533–7548. <https://doi.org/10.3390/molecules18077533>.

- Maleki, S., Falaki, F., Karimi, M., 2019. Synthesis of SDS micelles-coated Fe₃O₄/SiO₂ magnetic nanoparticles as an excellent adsorbent for facile removal and concentration of crystal violet from natural water samples. *J. Nanostructure Chem.* 9, 129–139. <https://doi.org/10.1007/s40097-019-0303-z>.
- Mamani, J.B., Gamarra, L.F., Brito, G.E., de, S., 2014. Synthesis and characterization of Fe₃O₄ nanoparticles with perspectives in biomedical applications. *Mater. Res.* 17, 542–549. <https://doi.org/10.1590/S1516-14392014005000050>.
- Manna, K., Panda, A.K., 2011. Physicochemical studies on the interfacial and micellization behavior of CTAB in aqueous polyethylene glycol media. *J. Surfactants Deterg.* 14, 563–576. <https://doi.org/10.1007/s11743-011-1261-8>.
- Matsui, I., 2005. Nanoparticles for electronic device applications: a brief review. *J. Chem. Eng. Japan* 38, 535–546. <https://doi.org/10.1252/jcej.38.535>.
- Menger, F.M., Portnoy, C.E., 1967. Chemistry of reactions proceeding inside molecular aggregates. *J. Am. Chem. Soc.* 89, 4698–4703. <https://doi.org/10.1021/ja00994a023>.
- Mészáros, R., Thompson, L., Bos, M., Varga, I., Gilányi, T., 2003. Interaction of sodium dodecyl sulfate with polyethyleneimine: Surfactant-induced polymer solution colloid dispersion transition. *Langmuir* 19, 609–615. <https://doi.org/10.1021/la026616e>.
- Mészáros, R., Varga, I., Gilányi, T., 2005. Effect of polymer molecular weight on the polymer/surfactant interaction. *J. Phys. Chem. B* 109, 13538–13544. <https://doi.org/10.1021/jp051272x>.
- Miyake, M., 2017. Recent progress of the characterization of oppositely charged polymer/surfactant complex in dilution deposition system. *Adv. Colloid Interface Sci.* 239, 146–157. <https://doi.org/10.1016/j.cis.2016.04.007>.
- Mukhopadhyay, A., Joshi, N., Chattopadhyay, K., De, G., 2012. A facile synthesis of PEG-coated magnetite (Fe₃O₄) nanoparticles and their prevention of the reduction of cytochrome C. *Appl. Mater. Interfaces* 4, 142–149.
- Nikas, Y.J., Blankschtein, D., 1994. Complexation of nonionic polymers and surfactants in dilute aqueous solutions. *Langmuir* 10, 3512–3528. <https://doi.org/10.1021/la00022a026>.
- Nikitin, A., Fedorova, M., Naumenko, V., Shchetinin, I., Abakumov, M., Erofeev, A., Gorelkin, P., Meshkov, G., Beloglazkina, E., Ivanenkov, Y., Klyachko, N., Golovin, Y., Savchenko, A., Majouga, A., 2017. Synthesis, characterization and MRI application of magnetite water-soluble cubic nanoparticles. *J. Magn. Magn. Mater.* 441, 6–13. <https://doi.org/10.1016/j.jmmm.2017.05.039>.
- Pham, X.N., Nguyen, T.P., Pham, T.N., Thuy, T., Tran, N., Tran, T.V.T., 2016. Synthesis and characterization of chitosan-coated magnetite nanoparticles and their application in curcumin drug delivery. *Adv. Nat. Sci. Nanosci. Nanotechnol.* 7, 045010.
- Pojják, K., Bertalanits, E., Mészáros, R., 2011. Effect of salt on the equilibrium and nonequilibrium features of polyelectrolyte/surfactant association. *Langmuir* 27, 9139–9147. <https://doi.org/10.1021/la2021353>.
- Prasad, C., Tang, H., Liu, W., 2018. Magnetic – Fe₃O₄ based layered double hydroxides (LDHs) nanocomposites – (Fe₃O₄/LDHs): recent review of progress in synthesis, properties and applications. *J. Nanostructure Chem.* 8, 393–412. <https://doi.org/10.1007/s40097-018-0289-y>.
- Raees, K., Ansari, M.S., Rafiquee, M.Z.A., 2019. Inhibitive effect of super paramagnetic iron oxide nanoparticles on the alkaline hydrolysis of procaine. *J. Nanostructure Chem.* <https://doi.org/10.1007/s40097-019-0308-7>.
- Raees, K., Ansari, M.S., Rafiquee, M.Z.A., 2018. Synergistic influence of inhibition of PEG-surfactant on the rate of alkaline hydrolysis of procaine. *J. Mol. Liq.* 257, 93–99. <https://doi.org/10.1016/j.molliq.2018.02.075>.
- Rahman, F., Rafiquee, M.Z.A., 2019. Influence of polyethylene glycol and surfactant mixed system on the rate of alkaline hydrolysis of benzocaine 111262. *J. Mol. Liq.* 291. <https://doi.org/10.1016/j.molliq.2019.111262>.
- Rehman, N., Khan, A., Bibi, I., Bica, C.I.D., Siddiq, M., 2013. Intermolecular interactions of polymer/surfactants mixture in aqueous solution investigated by various techniques. *J. Dispers. Sci. Technol.* 34, 1202–1210. <https://doi.org/10.1080/01932691.2012.739940>.
- Reichert, M.G., Butterworth, J., 2004. Local anesthetic additives to increase stability and prevent organism growth. *Tech. Reg. Anesth. Pain Manag.* 8, 106–109. <https://doi.org/10.1053/j.trap.2004.03.003>.
- Reuss-Lamky, H., 2007. Administering Dental Nerve Blocks. *J. Am. Anim. Hosp. Assoc.* 43, 298–305. <https://doi.org/10.5326/0430298>.
- Rodenas, E., Vera, S., 1985. Iterative Calculation Method for Determining the Effect of Counterions on Acetylsalicylate Ester Hydrolysis in Cationic Micelles 1981–1984. doi: 10.1021/j100249a029.
- Sanchez, L.M., Martin, D.A., Alvarez, V.A., Gonzalez, J.S., 2018. Polyacrylic acid-coated iron oxide magnetic nanoparticles: the polymer molecular weight influence. *Colloids Surf. A Physicochem. Eng. Asp.* 543, 28–37. <https://doi.org/10.1016/j.colsurfa.2018.01.050>.
- Santra, S., Tapeç, R., Theodoropoulou, N., Dobson, J., Hebard, A., Tan, W., 2001. Synthesis and characterization of silica-coated iron oxide nanoparticles in microemulsion: the effect of nonionic surfactants. *Langmuir* 17, 2900–2906. <https://doi.org/10.1021/la0008636>.
- Saranya, T., Parasuraman, K., Anbarasu, M., Balamurugan, K., 2015. XRD, FT-IR and SEM study of magnetite (Fe₃O₄) nanoparticles prepared by hydrothermal method. *Int. Res. J. Nano Sci. Technol.* 5, 149–154.
- Schramm, L.L., Stasiuk, E.N., Marangoni, D.G., 2003. Surfactants and their applications. *Annu. Reports Prog. Chem. – Sect. C* 99, 3–48. <https://doi.org/10.1039/B208499F>.
- Shaban Ansari, M., Raees, K., Rafiquee, M., 2018. Influence of surfactants/polyethylene glycols mixture on the kinetics of alkaline hydrolysis of tetracaine. *J. Mol. Liq.* 272, 638–644. <https://doi.org/10.1016/j.molliq.2018.09.129>.
- Shen, L., Qiao, Y., Guo, Y., Meng, S., Yang, G., Wu, M., Zhao, J., 2014. Facile coprecipitation synthesis of shape-controlled magnetite nanoparticles. *Ceram. Int.* 40, 1519–1524. <https://doi.org/10.1016/j.ceramint.2013.07.037>.
- Tromsdorf, U.I., Bruns, O.T., Salmen, S.C., Beisiegel, U., Weller, H., 2009. A highly effective, nontoxic T 1 MR contrast agent based on ultrasmall PEGylated iron oxide nanoparticles. *Nano Lett.* 9, 4434–4440. <https://doi.org/10.1021/nl902715v>.
- Wei, Y., Han, B., Hu, X., Lin, Y., Wang, X., Deng, X., 2012. Synthesis of Fe 3 O 4 nanoparticles and their magnetic properties. *Procedia Eng.* 27, 632–637. <https://doi.org/10.1016/j.proeng.2011.12.498>.
- Yue-jian, C., Juan, T., Fei, X., Jia-Bi, Z., Ning, G., Yi-Hua, Z., Ye, D., Liang, G., 2010. Synthesis, self-assembly, and characterization of PEG-coated iron oxide nanoparticles as potential MRI contrast agent. *Drug Dev. Ind. Pharm.* 36, 1235–1244. <https://doi.org/10.3109/03639041003710151>.